The Vertical Transport of Air Pollutants by Convective Clouds Part II: Transport of Soluble Gases and Sensitivity Tests①

Kong Fanyou (孔凡铀)
Department of Geophysics, Peking University, Beijing 100871
Received March 13, 1993; revised May 31, 1993

ABSTRACT

A two-dimensional, non-reactive convective cloud transport model is used to simulate in detail the vertical transport and wet scavenging of soluble pollutant gases by a deep thunderstorm system. Simulations show that for gases with not very high solubility, a deep and intense thunderstorm can still rapidly and efficiently transport them from boundary layer (PBL) up to mid and upper troposphere, resulting in a local significant increase of concentration in the upper layer and a reduction in PBL. Dissolution effects decrease both the incloud gas concentration and the upward net fluxes. The higher the solubility is, the more remarkable the decrease is. However, for very low soluble gases ($H < 10^2$ M atm^{-1}), the influences are very slight. In addition, the effects of irreversible dissolution and aqueous reactions in drops on the vertical transport of gaseous pollutants are estimated in extreme.

Key words: Gaseous pollutants, Pollutant transport, Convective transport, Numerical simulation of cumulus clouds, Wet scavenging

I. INTRODUCTION

Convective activities, as the most important vertical mixing mechanism in troposphere, play a significant role in vertical redistributions of pollutant gases or trace species. These redistributions, moreover, can largely increase the long-range transport abilities of the species and consequently affect the air quality of non-emission regions and global atmospheric chemistry. In order to obtain a complete view on the vertical transport process of gaseous pollutants by convective clouds and to provide a foundation for parameterizing the process in long-range pollutant transport models, a two-dimensional, slab-symmetric, fully elastic, non-reactive convective cloud transport model were developed in Part I of this study (Kong and Qin, 1993). In that paper, moreover, a preliminary simulation for the vertical transport of an initially negative-exponentially distributed, insoluble trace gas by deep storm had been made. For soluble gases, their dissolutions on hydrometeor particles undoubtedly have influences on the convective transport process. Some numerical simulation works have treated dissolution of soluble gases into cloud drops extensively (e.g. Hales and Dana, 1979; Hales, 1982; Chameides, 1984; Qin and Chameides, 1986). These researches, however, were focussed on wet scavenging and mainly involved with stratiform clouds. On the other hand, Chaumerliac et al.(1992) explicitly simulated the vertical transport and redistribution of

①The work is supported by National Post-Doctoral Science Foundation

atmospheric pollutant gases in the regions of frontal clouds by using a two-dimensional mesoscale meteorological model, and carried out sensitivity experiments on the influence of solubility. They came to the conclusion that the frontal ascending flow is effective in transporting the insoluble gases upward, and that, as solubility is getting larger, the pollutant gases could be bound in PBL.

This paper, as the second part in a series of researches, presents the vertical transport features of soluble pollutant gases by a deep convective thunderstorm system, discusses the relative importance of wet scavenging and its possible influences on the vertical transport, and carries out sensitivity experiments on solubility and treatment of gas uptaking by ice particles. Finally, the extreme effects of fully irreversible dissolution and aqueous reactions on the convective transport of gaseous pollutants are estimated.

II. SIMULATION CASES

The sounding data of the modeling thunderstorm's environment and the choosing of numerical integration parameters are all the same to those presented in Part I (Kong and Qin, 1993). No ambient wind is added. The two-dimensional simulating thunderstorm has a maximum cloud top of over 12 km AGL (above ground level), a peak updraft speed of about 20 ms^{-1}, and a lifetime longer than one hour. During 60 minutes of simulation, the storm produces 50 mm of maximum surface rainfall with a cover extent of 9 km. Of the total precipitation, the ice water accounts for 20%.

The initial pollutant gas distribution is assumed horizontally homogeneous with a maximum concentration of 10 ppbv at the surface and decrescent with height. By choosing different solubility coefficients, H, and different dissolving schemes, five cases are accomplish this paper. The general character and parameter of each case is listed in Table 1. According to the characters, these cases can be classified into three groups: AI1 is the pure gaseous (insoluble) transport case, which, already been presented in Part I, is used as a contrast case in this paper; AI2 and AI3 are the soluble pollutant gas transport cases, between which the solubility coefficients differ by one order of magnitude. The last group of cases, AE2 and AE3, is designed for a special purpose of estimating the influences of aqueous chemical reactions on the transport features of gaseous pollutants, which will be explained in detail in Section IV.

Table 1. General Characters of Simulating Cases

Case	AI1	AI2	AI3	AE2	AE3
H(M atm^{-1})	–	10^2	10^3	10^2	10^3
general character	insoluble pollutant gas (contrast case)	soluble gas, reversible dissolution, ice uptaking	soluble gas, reversible dissolution, ice uptaking	soluble gas, irreversible & instant full depletion	soluble gas, irreversible & instant full depletion

A part of numerical results of these cases are listed in Table 2 and Table 3. Since the modeling thunderstorm reaches its mature stage by 40 min and roughly remains steady afterwards, the 50-minute outputs are used in most of the following analyses.

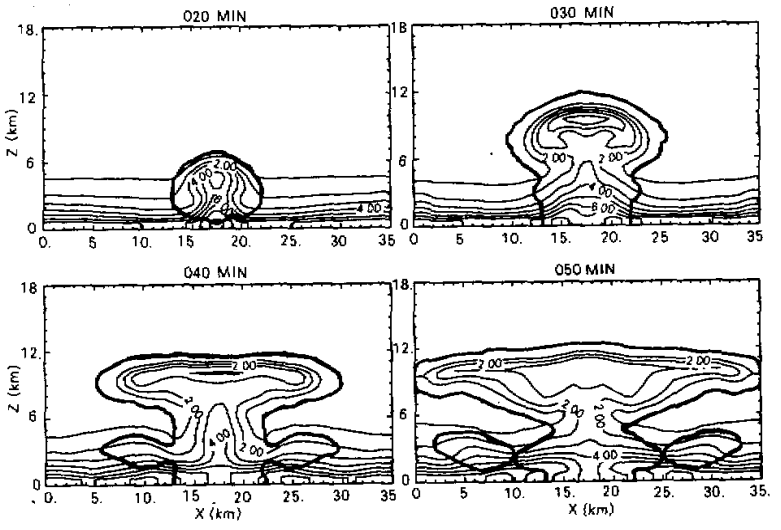

Fig. 1. Distribution of pollutant gas concentration (X_v) foe A13 in 10-minute intervals with a contour interval of 1 ppbv. The heavy solid line is the outline of the modeling storm's total hydrometeor field.

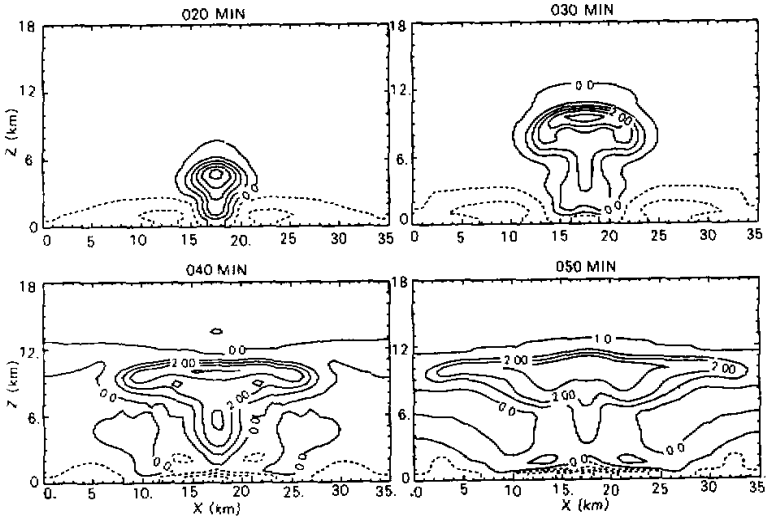

Fig. 2. Distribution of concentration deviation ($\Delta X_v = X_v - \overline{X}_v$) for A13 with contour interval of 1 ppbv. The dashed lines stand for negative values.

III. TRANSPORT OF SOLUBLE GASES

1. *General Transport Features*

AI3 simulates the transport of a soluble pollutant gas with $H = 10^3$ M atm^{-1} by the deep thunderstorm. Fig. 1 and Fig. 2 depict the pollutant gas concentration field (X_v) and the concentration deviation from environmental profile (ΔX_v) in time sequence, respectively. It is apparent that though in AI3 there is dissolution process, the principal transport results are qualitatively consistent with those in AI1 for insoluble gases (presented in Part I).

During the convective transport of soluble pollutant gases by thunderstorm, a part of gaseous content dissolves into cloud and rain drops, and a part of the dissolved content further transfers into ice particles. Fig. 3 presents the aqueous contents in cloud and rain water (X_c,X_r), and the equivalent contents in ice crystal and graupel or hail particles (X_i,X_g) at 40 min for AI3 case. It is evident that the equivalent concentration (mixing ratio) fields are well coincident with the corresponding hydrometeor fields in extent. The aqueous pollutant and the constituent bound in graupel or hail particles mainly appear in the layer below 9 km AGL. In the higher layer, only appears the equivalent content in ice crystal. In magnitude, however, each content in hydrometeor particles is very low with the maximum no more than 0.4 ppbv. This can also be seen in Table 2. At 50 min, the domain-wide sum of pollutant contents bound in hydrometeor particles for AI3 is only about 0.2 mol, being under 0.1% of the total pollutant mass (including gaseous). During 50-minute simulation, the modeling storm removes a sum of about 0.9 mol pollutant mass through precipitation scavenging, most of which is scavenged by rainfall. As compared to the total gaseous pollutant mass, this wet scavenging amount is still very slight, only accounting for 4%.

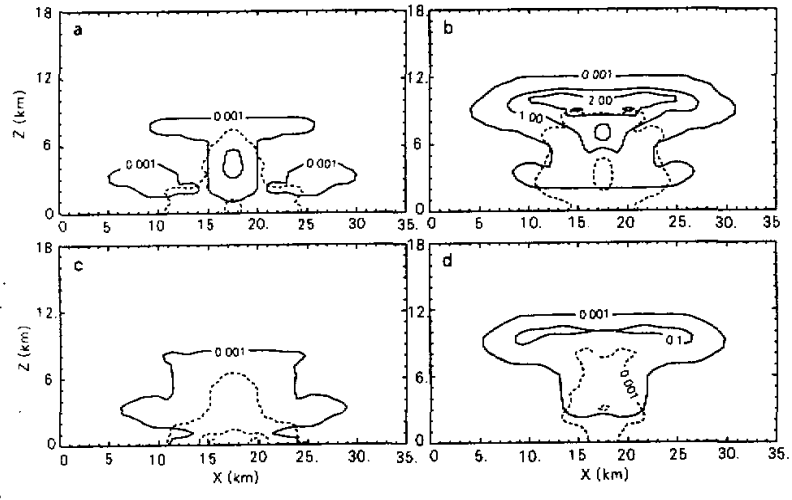

Fig. 3. Dsitribution of hydrometeor fields and pollutant constituents for AI3 at 40 min, (a) solid line for q_c, dashed line for q_r; (b) solid for q_i and dashed for q_g; (c) solid for X_c and dashed for X_r; and (d) solid for X_i and dashed for X_g. The contour interval in (a) and (b) is 1 g kg^{-1} starting from 0.001 g kg^{-1}, and that in (c) and (d) is 0.1 ppbv starting from 0.001 ppbv.

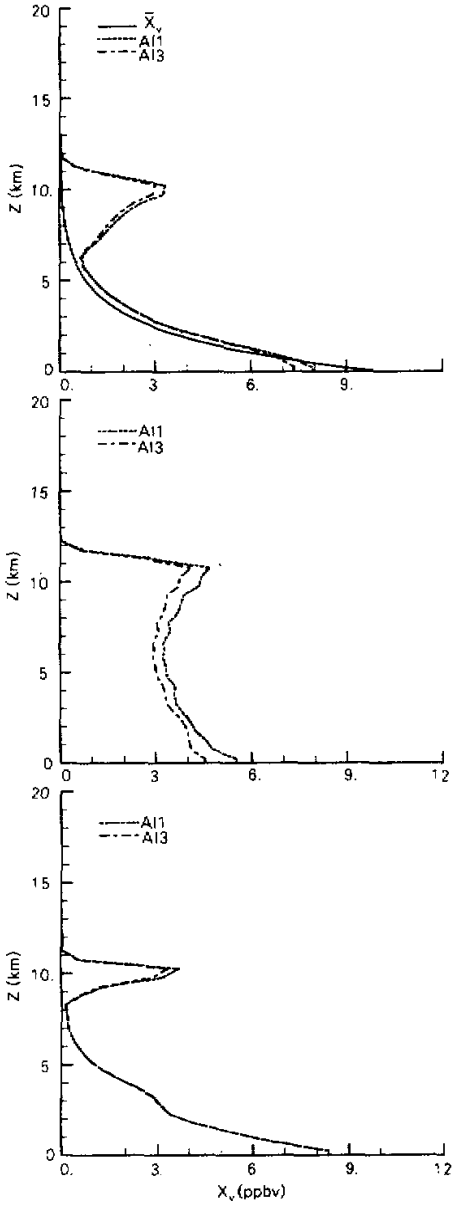

Fig. 4. Vertical profiles of X_v at 50 min. (a) domain-wide horizontal average with the solid line referring to initial profile; (b) local profiles in core area, x = 17.5 km; (c) local profiles in surrounding point of x = 4.5 km.

2. *Effects of Solubility on Transport*

AI1, AI2, and AI3 simulate, the transports of insoluble, soluble with $H = 10^2$ M atm^{-1} and soluble with $H = 10^3$ M atm^{-1} pollutant gases by deep thunderstorm, respectively. The intercomparison of these three cases made below is to reveal the influences of solubility of pollutant gases on the vertical transport features.

Fig. 4 depicts the vertical profiles of the gaseous pollutant concentration both in the core area and in the surrounding environment, and the horizontally averaged profiles, for AI1 and AI3 at 50 min. Since the profiles of AI2 closely coincide with those of AI1, they are omitted here. It can be seen that in the range of solubility specified in this paper, the redistribution features of gaseous pollutants caused by thunderstorm transport are quite similar to those of insoluble gases. In the storm's central area, the intense updraft flow causes the pollutant gas to become evenly distributed, with the upper bound of this even layer being near 12 km AGL and slightly below the storm top. As a result, the low-level concentration largely decreases whereas the concentration in middle and upper troposphere significantly increases (see Fig. 4b).

By comparing the two profiles of AI1 and AI3 in Fig. 4, it is easy to see that the dissolution process leads the gaseous pollutant concentration in the entire cloud layer to decrease, especially in the core area. Additionally, the larger the solubility is, the more significant the decrease is. In fact, the two concentration profiles of AI1 and AI2 close up each other, with exception in a very thin layer near surface. However, the concentration of AI3 can decrease by up to 18% in core area. The average concentration decrease resulted from dissolution is more significant both in anvil layer and in PBL.

Table 2 lists some statistical results of

each case during 50–minute integration, in which operator $\sum$ refers to a summation over all grid volumes in domain, $\sum X$ is the domain–wide total pollutant mass of all categories, $\Delta(\sum X) = \sum X - (\sum X)_0$, refers to the net increment of the domain pollutant mass. Here, $(\sum X)_0$ is the initial value and is equal to 17.422 mol for all cases in this paper. TFLUXB is the total flux of pollutant gas through lateral boundary. TSCAVL is the total scavenging mass of pollutant gas by rain drops, TSCAVI is the total pollutant mass scavenged by ice precipitation, TREACM is the total removed pollutant mass through instant reaction. These four quantities are all accumulated during the 50–minute simulation. In addition, the numerical errors in the pollutant mass budget are also listed in the table.

Table 2. Statistical Results during 50–Minute Simulation

case	AI1	AI2	AI3	AE2	AE3
$\sum X_v$ (mol)	22.503	22.313	21.520	21.044	17.477
$\sum X_c$ (mol)	0.0	0.004	0.035	0.0	0.0
$\sum X_r$ (mol)	0.0	0.001	0.035	0.0	0.0
$\sum X_i$ (mol)	0.0	0.011	0.104	0.0	0.0
$\sum X_g$ (mol)	0.0	0.002	0.027	0.0	0.0
$\sum X$ (mol)	22.503	22.331	21.721	21.044	17.477
$\Delta(\sum X)$ (mol)	5.08	4.91	4.30	3.62	0.055
TFLUXB (mol)	5.809	5.809	5.810	5.810	5.815
TSCAVL (mol)	0.0	0.381	0.821	0.0	0.0
TSCAVI (mol)	0.0	0.005	0.053	0.0	0.0
TREACM (mol)	–	–	–	1.154	4.787
numerical loss (%)	3.14	2.25	2.85	4.68	5.27

For AI2, the instantaneous value of total pollutant mass bound in the hydrometeor particles at 50 min is 0.018 mol, with most part in ice crystals. This mass only accounts for 0.08% of the total gaseous mass. The corresponding values for AI3 are 0.201 mol and 0.93%, respectively. The total wet scavenging pollutant mass is 0.386 mol for AI2 and 0.874 mol for AI3. Of these removal masses, most part is scavenged by rainfall. Adding up the accumulative wet scavenging mass and the instantaneous non–gaseous content, the total dissolving pollutant masses during 50 minutes are 0.404 mol for AI2 and 1.075 mol for AI3, accounting for 2.32% and 6.17% of the initial pollutant mass, $(\sum X)_0$, respectively. On the other hand, the low–level inflow air carries as high as 5.8 mol of pollutant gas into the domain, resulting in an increase of domain gaseous pollutant content by about 30%. In Table 2, the total gaseous pollutant contents $(\sum X_v)$ for AI1, AI2 and AI3 decrease successively. So do $\sum X$ and $\Delta(\sum X)$. In regard to degree, this decrease is not equally proportional to the solubility coefficient, H, for the deviation of AI3 from AI2 is much more significant than that of AI2 from AI1.

3. *Transport Flux Analyses*

Firstly, the simulation results of AI3 are used to analyze the net fluxes of soluble pollutant gas through some particularly specified planes in the thunderstorm system. Fig. 5

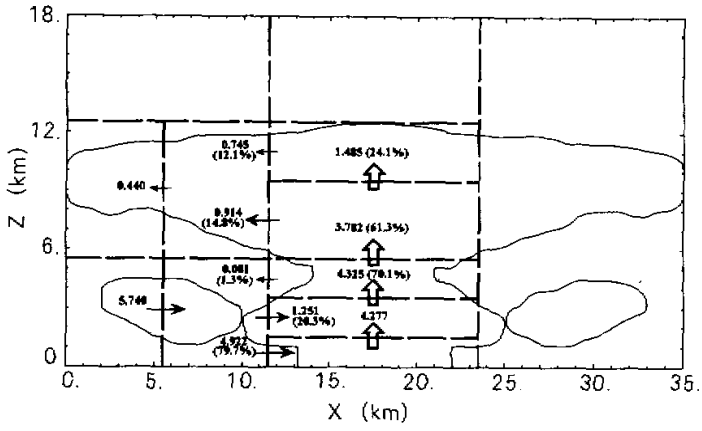

Fig. 5. Accumulative net fluxes of pollutant gas over 50 min for AI3. Arrows show directions of net fluxes and values in brackets represent percentages of relevant fluxes to the low-level net inflowing mass.

Table 3. Net Fluxes during 50-minute Integration (unit: mol)

case	AI1	AI2	AI3	AE2	AE3
0–3.5 km AGL into column	6.080	6.122	6.173	6.313	6.453
0–1.5 km AGL into column	4.825	4.870	4.922	5.081	5.243
	(79.4)	(79.5)	(79.7)	(80.5)	(81.2)
3.5–5.5 km AGL out column	0.083	0.083	0.081	0.088	0.086
	(1.4)	(1.4)	(1.3)	(1.4)	(1.3)
5.5–12.5 km out column	1.816	1.803	1.659	1.643	0.806
	(29.9)	(29.5)	(26.9)	(26.0)	(12.5)
5.5 km AGL upward within	4.135	4.111	3.782	3.722	1.935
column	(68.0)	(67.2)	(61.3)	(59.0)	(30.0)
9.5 km AGL upward within	1.632	1.620	1.485	1.435	0.687
column	(26.7)	(26.5)	(24.1)	(22.7)	(10.6)
5.5 km AGL domain-wide	4.118	4.093	3.765	3.703	1.918
upward					
5.5 km AGL domain-wide	141.2	140.3	129.1	127.0	65.8
mean rate (mol $km^{-2}h^{-1}$)					

* Values in brackets represent the percentages of the net inflowing pollutant mass of 0—3.5 km AGL.

shows these fluxes. Because of the model's two-dimensional, slab-symmetric geometric structure, the specified planes in the figure are of united thickness. In Fig. 5, the two vertical heavy dashed lines—surrounding column, with an extent of 12 km, represents the main storm portion. It can be seen from the figure that during the 50-minute simulation a total of 6.173 mol pollutant gas enters into the storm column with low-level inflow air, most from the layer below 1.5 km AGL. Of this low-level net inflowing mass, 70% (4.325 mol) is pumped upward, 61.2% (3.782 mol) is transported through the 5.5 km altitude, 24% (1.485 mol) is even carried

up to the layer above 9.5 km AGL. In anvil layer (from 5.5 to 12.5 km AGL), the net outflowing pollutant mass from the column is 1.659 mol, accounting for 27% of the low-level net inflowing pollutant mass. In middel layer (from 3.5 to 5.5 km AGL), there is a weak net outflowing flux through the column boundary, which may be the cause of mid-layer detrainment. Furthermore, Fig. 5 shows that the vertical transport pathway of gaseous pollutant is concentrated within the storm column, and the horizontal transport pathways are mainly located in PBL and in anvil layer. In the sense of long-term accumulative net flux, the vertical exchange out of the cloud column is slight. For example, the outside column net vertical flux through 5.5 km AGL is only 0.017 mol, with a downward-pointing direction.

Similar to the insoluble case in Part I, the net pollutant mass transported, over the entire domain scale, by the modeling thunderstorm up to the middle troposphere (above 5.5 km AGL) for AI3 case is calculated to be 3.765 mol, which is equivalent to a domain average vertical transporting rate of 129.1 mol km^2h^{-1}. The column average rate at the same altitude is 3 times of it, being 378.2 mol $km^{-2}h^{-1}$.

For the convenience of comparing the transporting fluxes among cases, the cumulative net fluxes through some principal planes (by reference in Fig. 5) for all simulating cases are collected together and listed in Table 3. From the first three columns of values in the table it is apparent that the influences of solubility on net fluxes have following characteristics. First, the dissolution process makes the low-level net inflowing pollutant mass increase, and the anvil layer net outflowing mass as well as the net upward fluxes within the storm column decrease. Second, as solubility increases, the change rates of above fluxes tend to enlarge, especially for the upper level outflowing fluxes and the vertical transporting fluxes within storm column. For these three cases, the ratios of the anvil layer net outflowing mass to the low-level net inflowing mass are 29.9%, 29.5%, and 26.9%, respectively, of which the percentage value of AI2 is slightly lower than that of AI1 whereas that of AI3 is 3 percentiles less

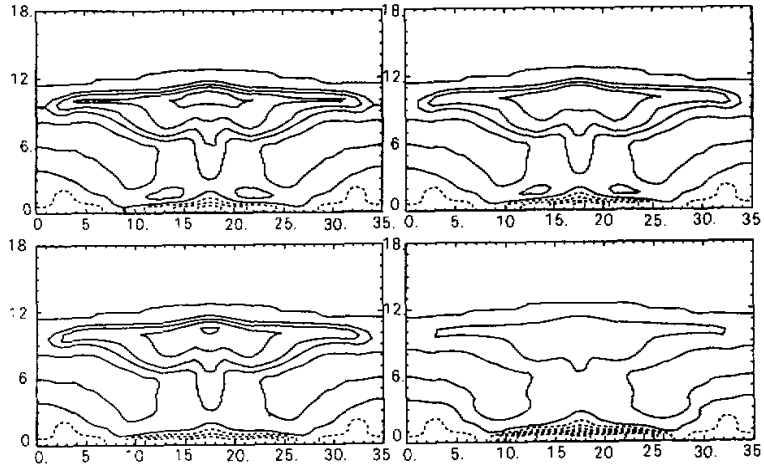

Fig. 6. Concentration deviation fields (ΔX_p) at 50 min for (a) AI2, (b) AI3, (c) AE2, and (d) AE3 cases, with a contour interval of 1 ppbv, dashed lines represent negative values.

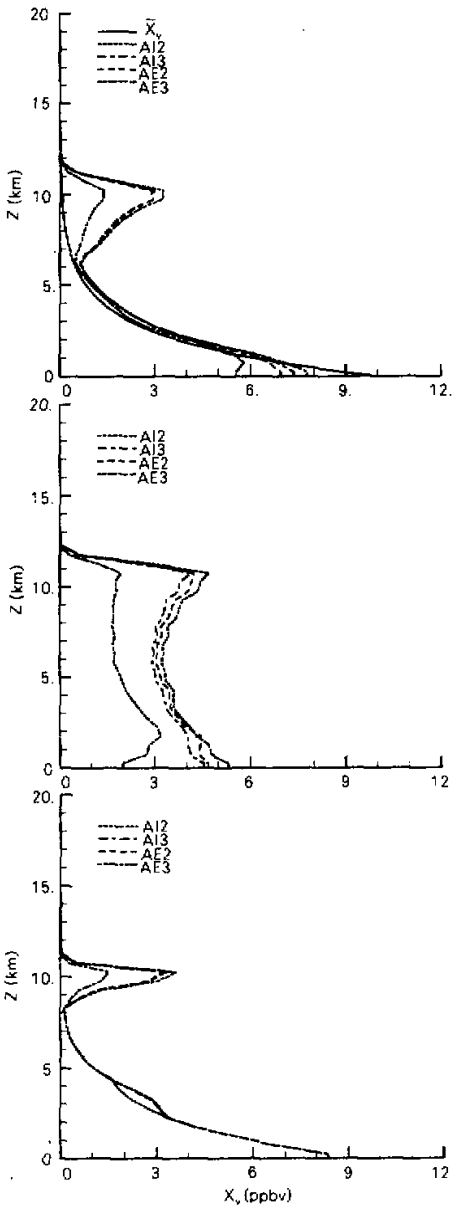

Fig. 7. Same as Fig. 4 but for AI2, AI3, AE2, and AE3.

than that of AI1. The ratios of the in-column net upward fluxes through 5.5 km AGL to the low-level net inflowing mass are 68%, 67.2%, and 61.3%, respectively, of which the percentage value of AI2 is only 0.8 percentiles less than that of AI1 whereas that of AI3 is reduced by 6.7 percentiles.

It should be noted that from the phenomenon that the low-level cumulative net flux of pollutant gas into the cloud column increases with the gas solubility, one can not deduce that the thunderstorm inflow has any enhancement. Dissolution of trace gases has no effect on the dynamics of modeling storm. In fact, the phenomenon is caused by the modification of the pollutant concentration in thunderstorm's cold outflow. At the boundary location of the storm column, the lowest 1-km layer is governed by the precipitation-deduced cold outflow after 40 min (see Fig. 2 in Part I). Since the pollutant concentration in storm column decreases in dissolution process, the amount of pollutant gas carried out of the column with low-level cold outflow correspondingly becomes less. As a result, the low-level cumulative net inflowing amount during 50 min is increased.

IV. INFLUENCES OF IRREVERSIBLE AQUEOUS-REACTION ON TRANSPORTS

Since this transport model does not treat aqueous reaction processes, the above involved pollutant gas dissolutions are assumed to be reversible. In fact, a dissolved constituent in liquid drops will be affected by dissociation and aqueous chemical reactions. As a result, the dissolution process should be irreversible. In order to estimate to what degree this irreversible dissolution would affect gaseous transport by using this reactionless model, specially designed cases, AE2 and AE3 are simulated in this section. They have the sameinitial conditions and parameters as AI2 and AI3, respectively, except that an instant-full-reaction scheme is adopted in treating dissolution process. This scheme, to be specific, assumes that all dissolving pollutant constituent into drops on one time step is

instantly depleted through aqueous chemical reactions within that step. Therefore, the so-called instant-full-reaction has two principal characteristics: i) The dissolution is fully irreversible, and ii) The dissolution process will continue until the pollutant gas in grid volume is fully depleted. It is quite evident that this much simplified scheme represents an extreme estimation. For many pollutant gases involving aqueous phase reactions, the dissociation processes after dissolution are fulfiled instantly (Xu and Qin, 1992), so the depletion rates in drops depend on the rates of aqueous phase reactions. Taking S(IV) as an example, the characteristic time of its oxidation reaction ranges from 10^2 to 1 for the concentration of aqueous H_2O_2 ranging from 1 to 100 μmol l^{-1}, which is within the integration time step Δt in this study. Therefore, the instant-full-reaction for SO_2 would be true only if a surpass of H_2O_2 remains in drops.

During model integration, the dissolving amounts of pollutant by cloud water and rain water accumulated over time and domain space are recorded, being referred to as total reactively removing mass, TREACM (Table 2). Fig. 6c-d are the pollutant gas concentration deviation fields ($\Delta X_v = X_v - \overline{X}_v$) at 50 min for AE2 and AE3. For the convenience of comparison, the corresponding fields for AI2 and AI3 are also depicted in Fig. 6a and Fig. 6b. It is apparent that the instant-full-reaction does not change the general distribution pattern of gas concentration but significantly reduce the concentration amount of each level. By comparing Fig. 6c with 6a and Fig. 6d with 6b we can find that the tendencies for both the extent and magnitude of the upper layer positive regions in AE group decrease, and for both the extent and magnitude of the low-level negative regions increase, which are especially significant in AE3 with higher solubility. The pollutant gas concentration profiles in different positions for these four cases at 50 min are presented in Fig. 7. It shows that the gaseous concentration in AE3 decreases to a very marked degree, the anvil layer concentration is less than half of that in AI3, and the lower portion of profile in core area even decreases downwards with a surface value of only 2 ppbv, being 2.5 ppbv lower than that in AI3 and 8 ppbv lower than the initial surface concentration. As regard to the domain horizontal average, the concentration in AE3 case is 1.4 ppbv at 10 km AGL, being 51.7% of that in AI3, and is 5.6 ppbv at surface level, 19.8% of that in AI3.

Some statistical results for AE2 and AE3 are also listed in Table 2 and Table 3. Table 2 shows that the total reactively removing pollutant amounts (TREACM) for both cases are more than the total dissolved pollutant masses for the AI group cases, for the ratios of AE2 to AI2, AE3 to AI3 are 4.787:1.075 and 1.154:0.404, respectively. For AE3, the TREACM is considerable, which has a value of 4.787 mol and roughly closes to the value of TFLUXB, causing the domain total pollutant amount not to change a lot from the initial value. In Table 3, we can find that the instant-full-reaction has larger influence on net fluxes, mainly lowering the upward transporting fluxes. For AE3, the upward fluxes of each level and the anvil layer outflowing fluxes are reduced by a factor of 2 as compared to those for AI3.

V. DISCUSSION AND CONCLUSIONS

In this paper, the researches are focused on the vertical transport and wet scavenging of soluble gaseous pollutants by a deep thunderstorm in stationary atmosphere, using a two-dimensional, reactionless cloud transport model. Since the emphasis is placed on the

transport features, the study only involves pollutant gases with not very high solubility ($H < 10^3 M\ atm^{-1}$). In atmosphere, the important pollutant gases within this range of solubility include NO_x, O_3, CO, CO_2, NH_3 and SO_2 etc, the vertical transports of these species play important roles in atmospheric chemistry. In addition to making contributions to long-range transport, NO_x, O_3, and CO, for example, can influence the upper troposphere photochemical reactions, while the SO_2 transported to upper level could contribute to the formation of sulphate aerosol in stratosphere. For those species with much higher solubility, such as H_2O_2, NO_3, and HNO_3, the results in this study may be less proper.

Simulations show that under the condition of reversible dissolution, the fully-developing deep thunderstorm is still efficient in vertically transporting soluble pollutant gases, being able to pump several tons of pollutant gases from PBL up to the anvil layer in mid and upper troposphere in a short time, forming an upper layer extensive local high concentration region and a concentration falling layer in PBL. The dissolution process leads both the gaseous pollutant concentration of each layer in storm and the net upward fluxes to more or less decrease. The higher the solubility is, the more significant the reduction is. However, for gases with solubility coefficients no more than $10^2 M\ atm^{-1}$, the dissolutions are very slight, exerting little influence on the vertical transport of pollutant gases. In this paper, when solubility coefficient is larger than $10^3 M\ atm^{-1}$, the dissolution effects become relatively evident. On the other hand, the gas dissolution effect leads the pollutant gas concentration in PBL to further decrease, which implies that besides the thunderstorm dynamic pumping, the wet scavenging has an additional contribution to the dilution of high concentrated pollutant gases in PBL, especially of those with higher solubility.

Aqueous chemical reactions in cloud could partially deplete the dissolving pollutant constituents, leading the dissolution process to be irreversible. In this paper, on an extreme assumption of instant-full-reaction, the most possible influences of aqueous reactions on the vertical transport features are estimated. The results indicate that, in extreme, the irreversibly dissolved pollutant amount is several times more than the reversibly dissolved amount, which results in a significant reduction of incloud gaseous pollutant concentration and causes the upward transporting pollutant amount in storm column to decrease by about 50%. Nevertheless, the general distribution pattern of pollutant gas concentration a concentration reduction in PBL and an increase in anvil layer is not changed. In the circumstance of chemical reactions, the concentration reduction in PBL is but more significant and the concentration increase in anvil layer is less significant.

REFERENCES

Chameides, W.L. (1984), Photochemistry of a remote marine stratiform cloud, *J. Geophys. Res.*, **89**: 4739-4755.

Chaumerliac, N. et al. (1992), The transport and redistribution of atmospheric gases in regions of frontal rain, *J. Atmos. Chemistry*, **14**: 43-51.

Hales, J.M. (1982), Mechanic analysis of precipitation scavenging using a one-dimensional, time-dependent model, *J. Atmos. Environ.*, **16**: 1775-1783.

Hales, J.M., and Dana, M.T. (1979), Precipitation scavenging of urban pollutants by convective storm systems, *J. Appl. Met.*, **18**: 294-316.

Kong, F., and Qin Yu (1993), The vertical transport of air pollutants by convective clouds. Part I: A non-reactive cloud transport model, *Adv. Atmos. Sci.*, **4**: 415–427.

Qin, Y., and Chameides, W.L. (1986), The removal of soluble species by warm stratiform clouds, *Tellus*, **38B**: 285–299.

Xu, L., and Qin Yu (1992), The parameterization of wet removal processes of gases under cloud base, *Environmental Chemistry* (in Chinese), **11**: 1–11.